

Wind Effects

New Frontier of Education and Research in Wind Engineering

Bulletin

Vol.13 April 2010

Wind Engineering Research Center
Graduate School of Engineering
Tokyo Polytechnic University

INDEX

● Professor Kareem Awarded with Member of the National Academy of Engineering	1
● The 6th International Advanced School (IAS6) on Wind Engineering was successfully held in Beijing, China	2
● International Forum on Tornado Disaster Risk Reduction for Bangladesh - To Cope With Neglected Severe Disasters.	4
● Report of "Seventh Asia-Pacific Conference on Wind Engineering (APCWE-VII)"	5
● Report on APEC-WW2009	6
● Reports on damage due to tornadoes in 2009 Results of post-disaster investigations	7
● Recent Topics of POD in Wind Engineering	17
● Vibration Control of Stay-Cable Using Magneto Rheological Damper	20

Professor Kareem Awarded with Member of the National Academy of Engineering

Ahsan Kareem, the Robert M. Moran Professor of Civil Engineering at the University of Notre Dame, was one of only 65 members inducted into the National Academy of Engineering (NAE) in its class of 2009 at a ceremony on October 4th in Irvine, California, where he was joined by his wife Gulrukh and son Danyal. Induction into the academy is reserved for those making outstanding contributions to "engineering research, practice, or education" and represents the highest professional honor in the field of engineering, reserved for just only 2000 of the 3 million engineers in the United States. It is a particularly high honor for Civil Engineers, with only 5 of this year's 65 inductees being from this discipline. As one of those five inductees, Prof. Kareem was formally honored for "*...contributions to analyses and designs to account for wind effects on tall buildings, long-span bridges, and other structures.*"

Professor Kareem graduated from the West Pakistan University of Engineering and Technology with distinction in 1968 and, through a joint program with the Massachusetts Institute of Technology, he earned his master's degree in structural engineering from the University of Hawaii. After completing his doctoral work under Jack Cermak at Colorado State University, Professor Kareem began his career in academia at the University of Houston, before moving to Notre Dame in 1990. Over a career spanning more than three decades, Professor Kareem has executed diverse research in the area of structural dynamics and in particular on the effects of wind on society. He has become an advocate for comprehensive national policies and design procedures to address wind hazards, leading to the incorporation of his design aids for wind loads into codes and standards both in the United States and abroad. These achievements

have earned him every major prize in wind engineering, including:

- the inaugural Alan G. Davenport Medal, presented by IAWE in recognition of his distinguished achievement in the dynamic wind effects on structures
- ASCE's Robert H. Scanlan Medal for outstanding original contributions to the study of wind-load effects on structural design, and
- ASCE's Jack E. Cermak Medal, named for Kareem's advisor, in recognition of his contributions to the study of wind effects on structures.

Professor Kareem also recently received ASCE's State-of-the-Art in Civil Engineering Award for his work on full-scale monitoring of tall buildings in Chicago and was presented on May 19, 2009 with the University of Notre Dame's Faculty Research Achievement Award. This award is bestowed on one of the university's faculty each year for universal recognition as a research leader in both past research accomplishments and future research potential.



The 6th International Advanced School (IAS6) on Wind Engineering was successfully held in Beijing, China

Date : August 31-September 4, 2009

Venue : China Academy of Building Research, Beijing, China

From August 31 to September 4, 2009, the 6th International Advanced School on Wind Engineering (IAS6) co-host by Global COE Program of Tokyo Polytechnic University (TPU) and China Academy of Building Research (CABR) was successfully held at CABR, Beijing, China.

The IAS6 invited 17 international distinguished professors in wind engineering field from 9 countries and regions to give their excellent lectures on respective research directions. They are:

Shuyang Cao (Tongji University, China)

Richard G.J. Flay (The University of Auckland, New Zealand)

Yaojun Ge (Tongji University, China)

Kenny C. S. Kwok (University of Western Sydney, Australia)

Partha Sarkar (Iowa State University, USA)

Ted Stathopoulos (Concordia University, Canada)

Yukio Tamura (Tokyo Polytechnic University, Japan)

Youlin Xu (The Hong Kong Polytechnic University, Hong Kong, China)

Lingmi Zhang (Nanjing University of Aeronautics & Astronautics, China)

Qingyan Chen (Purdue University, USA)

Richard de Dear (The University of Sydney, Australia)

Takashi Kurabuchi (Tokyo University of Science, Japan)

Xiaofeng Li (Tsinghua University, China)

Masaaki Ohba (Tokyo Polytechnic University, Japan)

Matthew Santamouris (University of Athens, Greece)

Michael Schatzmann (University of Hamburg, Germany)

Ryuichiro Yoshie (Tokyo Polytechnic University, Japan)

The IAS6 was also regarded as an import international academic activity to China wind engineering society



as well as to CABR this year. The president of IWEA, Prof. Yukio Tamura of TPU, the president of China wind engineering committee, Prof. Yaojun Ge of Tongji University and the president of CABR, Prof. Jun Wang attended the IAS6.

The IAS6 received warm responses from related colleges and academic organizations in China. It attracted totally about 80 postgraduate students and young researchers to attend, who came from 22 colleges and institutes, mainly from Tongji University, Beijing Jiaotong University, Harbin Institute of Technology, Shanghai Jiaotong University, Zhejiang University, Peking University, South China

University of Technology and CABR etc..

The 5 day's systematic lectures were divided into two parts: Structural Wind Engineering and Environmental Wind Engineering, and totally 19 ones were given. The involved fields included: wind hazards and extreme wind climate, wind loads of buildings and structures, urban wind environment, CFD numerical simulation and wind tunnel test, outdoor wind environment comfort and indoor ventilation/thermal comfort, urban air pollution and dispersion etc.. They almost included all the important research aspects in the field of wind engineering. On

and after the lectures, the young students discussed the problems interested positively.

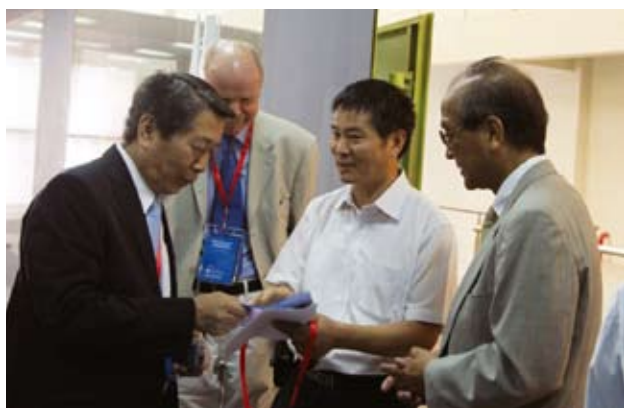
On August 31, the vice president of CABR, Prof Lin Haiyan and the general engineer, Prof. Zhao Jida attended the opening ceremony as the host, and Prof. Lin gave a short address to welcome all the lecturers and students.

On September 2, the president of CABR, Prof. Wang Jun interviewed with the IWEA president Prof. Tamura and all the lecturers. He expressed the appreciations to all the invited lecturers, and also expressed a wish for strengthening the cooperation of CABR with international scholars in the research field of wind engineering.

During the break between two parts, the invited lecturers and students visited the newly constructed large-scale boundary layer wind tunnel lab, which were two sections 6m *3.5m and 4m*3m respectively.

On September 4, Prof. Michael Schatzmann and Prof. Richard de Dear gave a warmhearted speech in the farewell banquet as the representatives of all invited lecturers.

The IAS6 was successfully held and closed through the intensive cooperation between the Wind Engineering Research Center of TPU led by Prof. Tamura and the Center of Wind Engineering Research of CABR led by Prof. Jin Xinyang. Many students wrote emails to the organizers of CABR to express their congratulations and appreciations after the IAS6. Through IAS6, it set up a bridge of friendship between the Chinese young students and international scholars.



International Forum on Tornado Disaster Risk Reduction for Bangladesh - To Cope With Neglected Severe Disasters.

“The International Forum on Tornado Disaster Risk Reduction for Bangladesh - To Cope With Neglected Severe Disasters” was held in Bangladesh on 13-14 December, 2009 at the Hotel Sheraton. Over one hundred seventy people attended, including a large number of international experts from the USA, Japan, Switzerland, Thailand and China. While Dr. Muhammad Abdur Razzaque, the Honorable Minister of Ministry of Food and Disaster Management, was the Chief Guest, Mr. Tamotsu Shinotsuka, Ambassador of Japan in Bangladesh, Prof. Dr. M.S. Akbar MP, Chairman of Bangladesh Red Crescent Society, and Mr. BMM Mozharul Huq, Advisor, Humanitarian Response Team, UNDP were present as Special Guests. Chaired by Prof. Yukio Tamura, IAWE President/TPU Global COE Director, the forum was addressed by Mr Salvano Briceno, Director of UNISDR and Mr. Tokiyoshi Toya, Director of WMO as guests of honor. Mr. Muhammad Saidur Rahman, Director, BDPC presented the welcoming address and Mr. Farhad Uddin, DG DMB proposed the vote of thanks from the local organizers.

The event was co-organized by Tokyo Polytechnic University Global COE Program TPU/GCOE, the Government of Bangladesh (Disaster Management

Bureau, Ministry of Food and Disaster Management, Meteorological Department, Ministry Of Defence), the Bangladesh Disaster Preparedness Centre (BDPC) and the International Association for Wind Engineering (IAWE).

Through a number of sessions addressed by key international and local experts, the forum captured severe local storm disaster risks in Bangladesh, raised awareness of risks at local, national, and international levels, and developed a strategy for reducing the risks through active interactions among renowned international experts, national and local experts, and local practitioners and decision makers. This strategy includes components of early warning systems; risk and vulnerability assessment; research on meteorology, climatology, and engineering; household and community shelter; public awareness and education; finance and community planning; and governance and policy making. The outcomes of this forum will help the Government of Bangladesh to adopt policies and develop planning to reduce risks from severe local storms. The outcomes will stimulate donor agencies and NGOs to implement specific projects to reduce disaster risks. Overall, the forum will contribute to the implementation of the Hyogo Framework for Action.



Report of “Seventh Asia-Pacific Conference on Wind Engineering (APCWE-VII)”

Date: November 8-12, 2009

Venue: The Grand Hotel, Taipei, Taiwan

The Seventh Asia-Pacific Conference on Wind Engineering (APCWE-VII) was held in The Grand Hotel (See Picture 1), Taipei, Taiwan over five days from November 8 to 12, 2009. APCWE is a regional conference of IAWE and is held every 4 years. There were about 220 participants from 19 countries, including 30 from Japan. Three keynote speeches and five invited lectures were scheduled. (Unfortunately, one invited lecture was canceled, so only were given.) The titles of the Keynote Speeches and Invited Lectures are outlined below:

[Keynote Speech]

- Wind-Induced Damage to Buildings and Disaster Risk Reduction (Professor Yukio Tamura)
- Targeted Observation of Tropical Cyclones (Professor Chun-Chieh Wu)
- The Changing Dynamics of Aerodynamics: New Frontiers (Professor Ahsan Kareem)

[Invited Speech]

- Wind and Structural Monitoring of Long Span Cable-Supported Bridges with GPS (Professor You-Lin Xu)
- Advances and Challenges in Applied Flow and Dispersion Modelling (Professor Bernd Leitl)

- Large Eddy Simulation on Building Aerodynamics (Professor Tetsuro Tamura)

- Development of Codification of Wind Loads in the Asia-Pacific (Dr. John D. Holmes)

There were 21 technical sessions: Bridge Aerodynamics, Wind Environment/Human Comfort, Aero-Elasticity, Field Measurement and Health Monitoring, Newly Developed Testing Facilities and Techniques for Wind Engineering Applications, Hazard Assessment, Low-Rise Buildings, Computational Wind Engineering, High-Rise Buildings, Wind Energy and Applications, Wind-Induced Structural Response, Environmental Dispersion, Bluff Body Aerodynamics, Wind Characteristics, Urban Flow and Dispersion Modeling, Cable Aerodynamics, Wind Loading, Wind Tunnel Tests/Industrial Applications, Experimental Modeling/Wind Tunnel Tests, Wind Coding Issues, Windborne Debris, Codification of Wind Load Vehicle, Wind Barrier and Sports and Indoor Air Quality and Ventilation. Each technical session was very informative and it was very difficult to select which session should be attended. The next APCWE (APCWE-VIII) will be held in India, 2013.



Picture 1 The Grand Hotel, Taipei



Picture 2 Participants for APCWE-VII (by courtesy of APCWE-VII Secretary)

Report on APEC-WW2009

The Fifth Workshop on Regional Harmonization of Wind Loading and Wind Environmental Specifications in Asia-Pacific Economies was held in Taiwan from Nov.12-14, 2009. The workshop was co-hosted by the Wind Engineering Research Center of Tamkang University and the Global COE Program of Tokyo Polytechnic University, and was aimed at harmonizing structural loading standards/codes and blending bylaws/specifications with wind environmental problems in the APEC region. Embracing new members from Canada, Sri Lanka, Nepal and Macau, a total of 31 experts from 18 countries and economies, attended the workshop.

The opening ceremony of the APEC-WW2009 was held on the afternoon of Nov. 12 at the APCWE7 venue, which is another important event in the field of wind engineering. After the welcoming speech by the Workshop Chairman, Prof. Chii-Ming Cheng, Prof. Yukio Tamura (Tokyo Polytechnic University, Japan) gave a speech



Photo 1. Venue of APEC-WW2009 at Tamkang University

emphasizing the importance of Wind Related Disaster Risk Reduction. Dr. John Holmes (JDH Consulting, Australia) presented a talk on design wind speeds in East Asian countries. The main event of APEC-WW2009 was held in the Lanyang campus at the Tamkang University from Nov.13-14. All member countries/economies presented reports on the development of wind engineering related archives in their countries. Resulting discussion clarified the current status of wind load standards of all countries and discrepancies among various countries' codes.

On Nov.14, the participants were divided into two groups to discuss the wind load and wind environment problems individually. In the wind load discussion group, wind load calculation results for three examples (low-rise, medium-rise and high-rise buildings) were confirmed. It was also agreed to include the WRDRR as a topic in the next event of APEC-WW. In the wind environment discussion group, knowledge on outdoor air pollutants and indoor air quality criteria were exchanged to provide further transparency and operational efficiency. In addition, benchmark tests on pollutant dispersion and urban ventilation should be carried out.

Resolutions on wind load and wind environment issues were achieved as the output of the workshop. Related documents can be downloaded from the official website of APEC-WW at <http://www.wind.arch.t-kougei.ac.jp/APECWW/>. It was decided to hold the next APEC-WW workshop in Korea in 2010.



Photo 2. APEC-WW2009 Group Photo

Reports on damage due to tornadoes in 2009 Results of post-disaster investigations

Rei Okada, G. R. Sabareesh, Akihito Yoshida, Masahiro Matsui, Cao Shuang, and Yukio Tamura
WERC, Tokyo Polytechnic University

1. Tornadoes and other gusty winds in 2009

Based on the JMA, 77 gusty winds were observed in Japan in 2009. Of the total, 24 were tornadoes, 4 were down bursts, 3 were gust fronts, 26 were water spouts, and 20 were unknown phenomena. Major tornadoes, gust fronts and down burst are shown in Fig. 1.

Members of our Global COE program went to 5 disaster areas to investigate damage due to tornadoes (red squares in Fig. 1).

This report describes the results of these field surveys. We mainly focused on damage to structures such as buildings, factories, dwellings and so on.

2. Tatebayashi Tornado

[Investigators: Rei Okada, Seizo Kawana, Masahiro Matsui]

On July 27, an F1 or F2 class tornado struck Tatebayashi city in Gunma prefecture. Based on data from the Amedas facility, the temperature decreased from 32 degrees C to 24 degrees C within 20 minutes, the maximum instantaneous wind velocity was 16.1m/s at 14:20, and the wind direction rapidly changed from North to South when the tornado struck, as shown in Fig. 2. Data from Amedas captured the characteristics of the tornado. (The distance between the damaged area and Amedas station was around 1.0km). The moving velocity of the tornado was 45km/h based on Japan Weather Association data.

The GCOE Program carried out a damage investigation

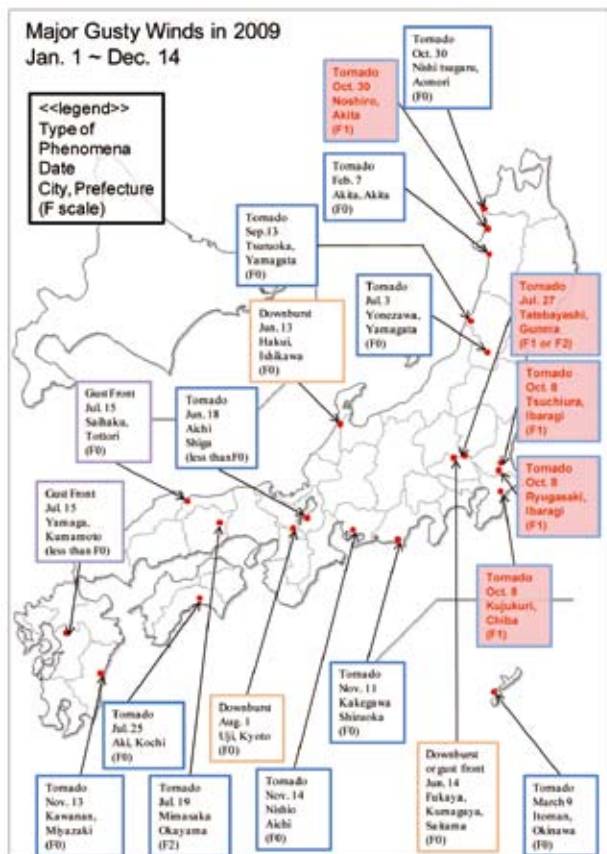


Fig. 1 Gusty winds in 2009

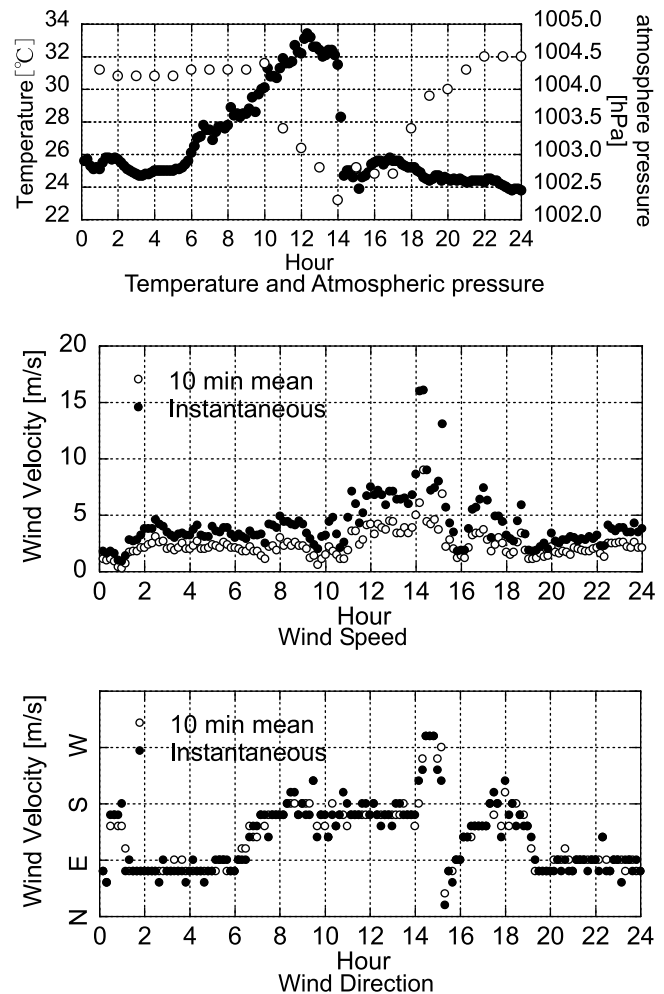


Fig. 2 Meteorological Data (Diurnal Change in July 27)

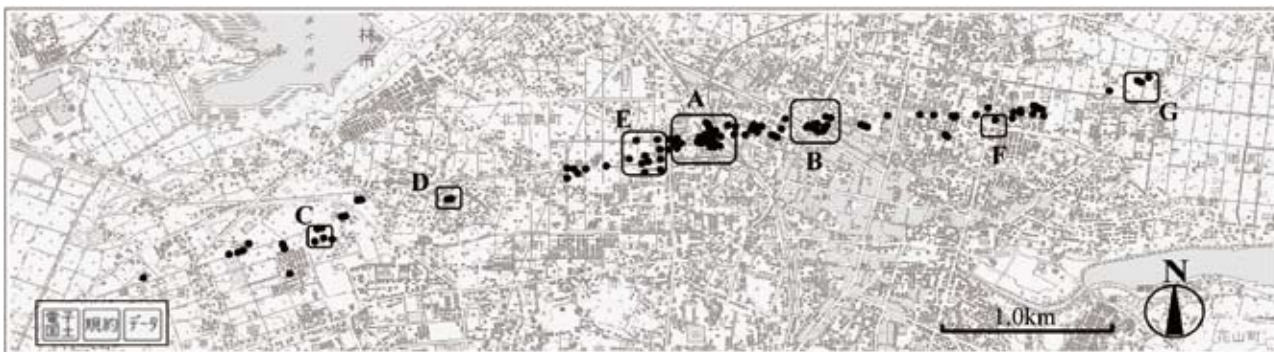


Fig.3 Overview of damage area

Table 1 Damage statistics (by Tatebayashi-city)

Human Suffering	Seriously-injured person	1
	Slightly-injured person	20
Dwelling Suffering	Complete collapse	14
	Half collapse	24
	Partially collapse	286
Non-dwelling Suffering	Complete collapse	11
	Half collapse	9
	Partially collapse	75
Car Suffering	Complete collapse	4
	Half collapse	14
	Partially collapse	15



d. Damaged wall and window due to debris (point A)



a. Damaged window of gymnastic hall (point C)



e. Damaged power pole due to debris (area A)



b. Wall of factory was flown away (point D)



f. Damaged cladding (area A)



c. Fallen crane and fence (point A)



g. Complete-collapsed storage (point F)
Fig. 4 Characteristic damage due to tornado

on this tornado on July 28. It was found that damage was distributed in a line running from west to east. The width and length of the damaged area were 50m and 6.5km, respectively (the locations of damage due to the tornado are shown in Fig. 3).

The most severe damage was concentrated in Shin-sakae town (area A in Fig. 3). Damage was also distributed in Nishimoto town (B), Ohtani town (C), Narishima town (D), Setoya town (F), and Wakamiya town (G), etc.

Damage statistics due to this tornado, based on an investigation by Tatebayashi-city, are shown in Table 1.

Fig.4 shows the pictures of major damages due to the tornado. The tornado touched down at Ohnishi town, and moved east. The windows of a gymnastic hall were broken by the wind pressure (Fig. 4a). On the same campus, there was damage to fences at point C. The roof and walls of a factory were broken by wind pressure and walls and roofs flew in an easterly direction. The tornado then moved through a residential area (Fig. 4b). Damage to electric poles, windows, walls, and solar panels due to debris were observed (Fig. 4d, e). Roof panels, claddings, structural frames etc were also damaged due to wind pressure (Fig. 4f, g). Next, the tornado moved to a rural area, and there was damage to green houses, etc.

3. Typhoon induced tornadoes due to Typhoon MELOR

3.1 Overview of Typhoon MELOR

Typhoon MELOR formed in the Marshall Islands on September 29, 2009. It made landfall on the Chita

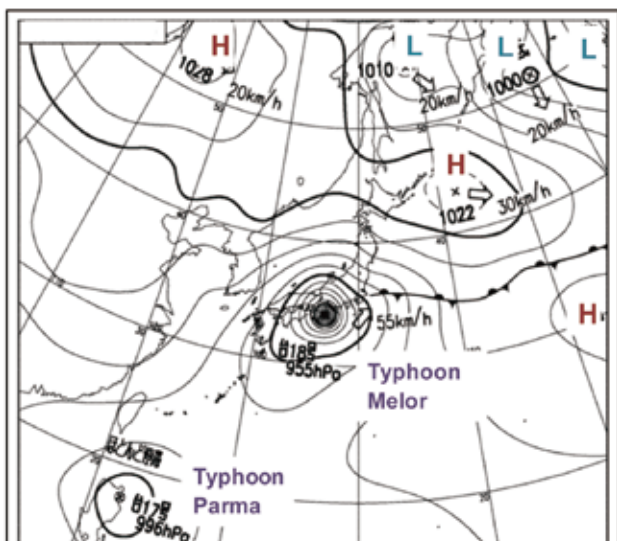


Fig. 5 Weather chart at 3AM, Oct. 8 (by JMA)

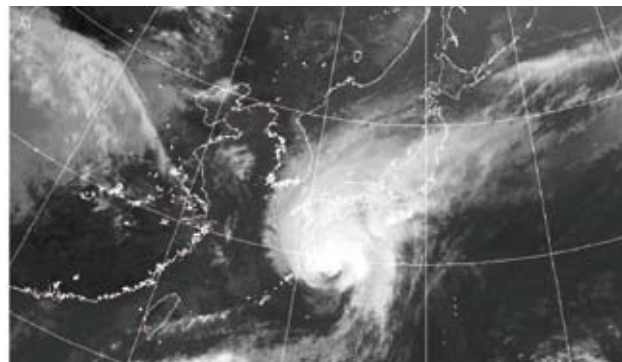


Fig. 6 Satellite image at 4:30 AM, Oct. 8 (by JMA)

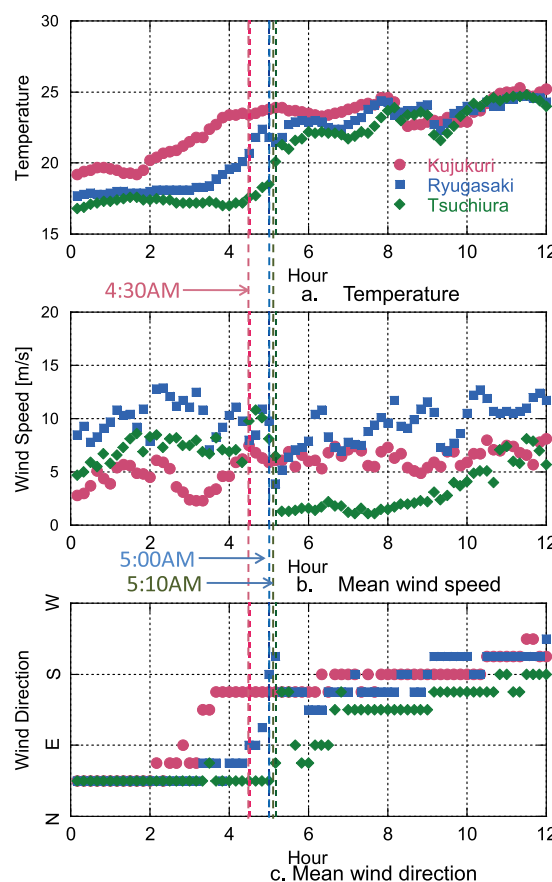


Fig. 7 Climate data [Diurnal change in Oct. 8]

Peninsula in Aichi Prefecture after 5 AM JST on October 8.

Concurrently with the landfall, 3 tornadoes occurred in the Kanto Area at Kujukuri city in Chiba prefecture, Tsuchiura city in Ibaragi prefecture, and Ryugasaki city in Ibaragi prefecture. This section reports damage due to typhoon-induced tornadoes related to typhoon MELOR.

Figs. 5 and 6 show the weather chart at 3AM and a satellite image at 4:30AM.

Fig. 7 shows climate data measured at the nearest Amedas weather station. The distances between the

weather station and the damaged areas were 20 km to Kujukuri, 1 km to Ryugasaki, and 4 km to Tsuchiura. Fig. 7 also shows the occurrence times.

In Tsuchiura and Ryugasaki, as shown in Fig. 7a, temperatures increased and wind direction changed rapidly from NE to S around the occurrence time. The wind speeds had local maximum values at the time the tornado occurred. However, temperature and wind direction changed gradually in Kujukuri because of the distance between the weather station and the damaged area. It was difficult to grasp the effect of the tornado on Kujukuri from the nearest weather station. Also at this time, typhoon MELOR made landfall on Honshu Island, so the effect of the typhoon became dominant. The presence of these tornadoes was made apparent by the warm and humid air flow due to the typhoon.

Table 2 shows the damage statistics due to the typhoon MELOR. These values are quick estimations by the Cabinet office of the Japanese government on September 16.

Fig. 8 depicts the area damaged by 3 typhoon-induced tornadoes (red squares in Fig. 8). The occurrence times of the tornadoes are also shown. On the morning of October 8, our Global COE program decided to dispatch survey missions to the damaged areas in Kujukuri, Ryugasaki, and Tsuchiura. On this morning, the Kanto region was hit by powerful winds and rain due to typhoon MELOR, which caused damage and disrupted public transportation. The Ryugasaki group departed for the damaged area by car, so the investigation was started at noon on October 8. The other 2 groups moved into the damaged areas by public transportation, so they arrived on the evening of October 8, and they started their damage investigation on the morning of October 9.

3.2 Ryugasaki tornado

[Investigators: Akihito Yoshida, Kim Yongchul]

As stated in the last section, on October 8, an F1 class tornado struck Ryugasaki city in Ibaragi prefecture.

We carried out a damage investigation of this tornado on October 8. The width and length of the damaged area were 200m and 4.0km, respectively. The distributions of damaged structures are shown in Fig. 9.

It was found that damage was distributed in a line running from south to north. The figure also shows the locations of the nearest Amedas Station. The damage is summarized as follows, based on the report of the

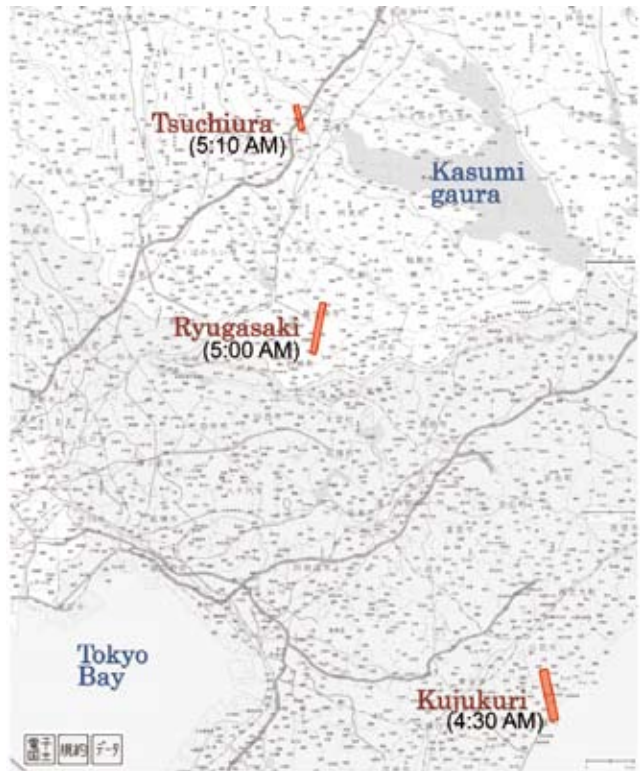


Fig. 8 Locations of damage area by 3 typhoon-induced tornadoes

Table 2 Damage statistics

Human Suffering	Dead person	41
	Missing person	4
	Seriously-injured person	205
	Slightly-injured person	1096
Dwelling Suffering	Complete collapse	109
	Half collapse	848
	Partially collapse	42183

Ryugasaki-city office and the Inashiki fire headquarters released on October 10. 4 people were injured, 13 non-dwellings had completely collapsed, 5 dwellings and 1 non-dwelling had half collapsed, 109 dwellings and 26 non-dwellings had partially collapsed, and 19 cars were destroyed.

Fig. 10 shows the major damage due to the tornado in Ryugasaki city. Fig. 10a shows some roof tiles on the leeward side blown off. Fig. 10b shows a collapsed garage. Structural members were also damaged and collapsed. The roof panels of a neighboring dwelling had also fallen off. Fig. 10c shows an overturned storage building. The major reason for this damage was corroded steel columns.

The roof panel and trusses blew off immediately after the upstream-located window broke. The shutter of



Fig. 9 Distribution of damage due to tornado (●)

window was not closed when the tornado struck.

3.3 Tsuchiura tornado

[Investigators: Shuang Cao, G. R. Sabareesh]

A tornado like wind outbreak was reported at around 5am on October 8 2009 in Tsuchiura, in the southern part of Ibaraki Prefecture, Japan. There was major and minor damage to around 60 residential buildings. Damage to property and crops was also notable, but there were



a. Damage to roof tiles



b. Collapsed garage



c. Wall and roof are partially overturned



d. Window was broken and Roof structure blown off



e. Inclined fences (damaged part described as yellow line)



f. Damaged roof tiles

Fig. 10 Major damage due to tornado in Ryugasaki

no human fatalities. The tornado can be classified as a less intense F1 type tornado based on the intensity of damage. On October 9 and 11, a Global COE team from TPU visited the areas of the reported tornado-like wind outbreak and found residential buildings with broken roofs and windows.

Two buildings at the touch down point, a Post Office and a residential building, suffered severe damage, as shown in Fig.11. The roofs of these two buildings were destroyed. Vehicles in the parking area surrounding the touchdown point were subjected to serious damage.

The tornado was found to head in an East-North-East direction, as observed from the damage to buildings and falling of poles. It had cut a path 1.5km long and about 40 m wide.

There was extensive damage to tiled roofs of single storied residential buildings. The team also observed dominant openings created on building envelopes after breakage of windows and doors due to flying debris. Fig. 12 shows an uprooted sign pole in the path of the tornado.

Typical tornado-like damage patterns were observed throughout the impact area, such as blown-off roof tiles and blown-out windows but undamaged walls. Trees and barricades on the path were knocked down. Fig.13 shows an uprooted tree in the tornado's path. Fig. 14 shows wall claddings damaged by debris. Car garages and green houses all along the tornado's path were severely

damaged (Figs. 15 and 16)

The damaged area was found to extend in a line from the touchdown point. Fig.18 shows the footprints of damage to buildings. As the tornado moved, it could have intensified, as is evident from the destruction of buildings numbered 20-43 in Fig. 14, and then its intensity may have reduced. At the end of its path, around the location of buildings 10-11, its severity decreased and damage was limited to a narrow area and petered out past building 14. Debris was found scattered around the regions of buildings 16-17 and also in a small irrigation canal in fields adjacent to building 15.



Fig. 13 Tree uprooted in tornado's path



Fig. 11 Roof tiles of residential building blown away at touchdown point



Fig. 14 Cladding damaged due to debris



Fig.12. Sign pole uprooted in tornado's path



Fig. 15 Damaged roof of car garage

3.4 Kujukuri tornado

[Investigators: Akihito Yoshida, Rei Okada, Le Thai Hoa, Kim Yongchul]

The scale of this tornado was F1. No people were injured, but 61 dwellings and 53 non-dwellings were completely, half, or partially collapsed. The TPU GCOE Program carried out a damage investigation on



Fig. 16 Damaged green house



Fig. 17 Wall of steel structure blown away

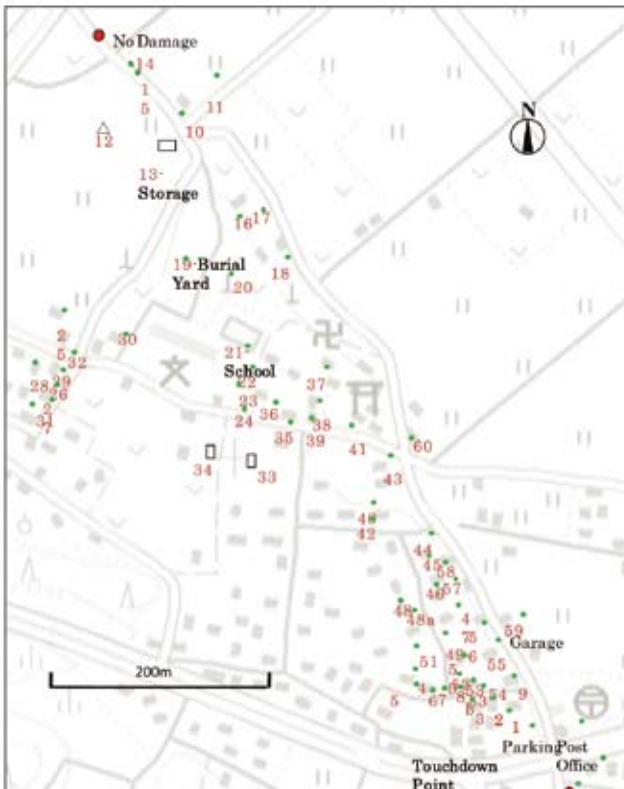


Fig. 18 Damage foot print

this tornado on Oct. 9. It was found that damage was distributed in a line running from south to north. The width and length of the damaged area was 20m and 4.1 km. The locations of damage due to the tornado are shown in Fig. 19.

The most severe damage was concentrated in the Sakuta area (area A in Fig. 19). This area is a residential

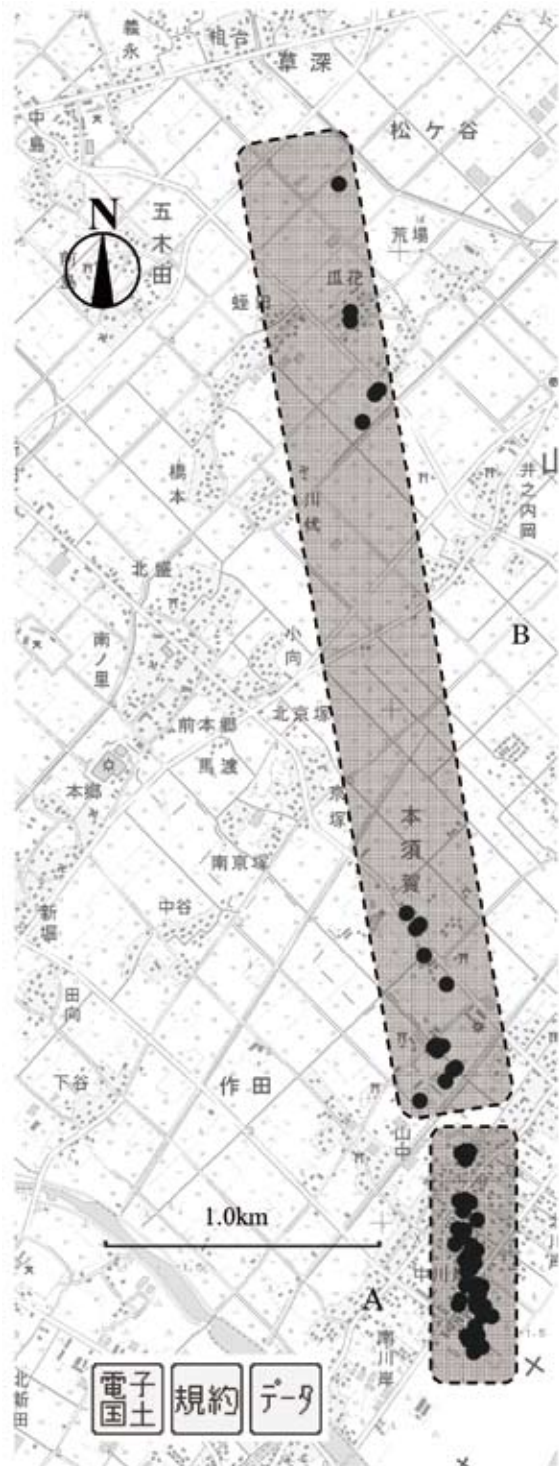


Fig. 19 Overview of damage

area. Area B is a rural area. In area A, dwellings (roofs, windows, walls, antennae, fences) were mainly affected by gusty wind. In area B, agricultural structures and facilities (such as green houses, storage facilities, cultivating machinery) were damaged. Fig. 20 shows the major damage due to the tornado.

4. Noshiro Tornado

[Investigators: Rei Okada, G. R. Sabareesh]

A tornado outbreak was reported on the morning of October 30 at Asanai, Noshiro City, Akita prefecture,



a. Half collapsed dwelling (area A)



b. Damaged cars (area A)



c. Damaged wooden cow house (area A)



d. Storage tipping damage (area A)



e. This dwelling was lifted up and down instantaneously by tornado (area A))



f. Damaged Roof truss (area B)



g. Damaged green house (area B)
Fig. 20 Major damage due to tornado

located in the north-west part of Japan. A two-man team from Tokyo Polytechnic University visited the affected areas the next day. This report summarizes some of the damage footprints based on a ground survey and the local environment situation on the morning of October 30 based on data received from the Japan Meteorological Agency (JMA). Fig. 21 shows a satellite image of the north part of Japan.

Well-developed thunderclouds can be observed above the damaged area (white arrow). These thunderclouds show strong association with the tornado.

The damage path was restricted to around 1km whereas debris could be found at distances up to 3.1km from the touchdown point (Fig. 22). The reported downfall time was around 9 AM. The damaged area was around 100m wide. Maximum instantaneous wind speed at the nearest AMEDAS station was 13.2m/s (Midori cho, Noshiro city).

The tornado's path had few residential buildings. Around 60% of its track comprised farmland. Thus, there was little damage to residential buildings. The few buildings that were in the path either collapsed partially or suffered severe damage. 6 residential and 23 non residential buildings were damaged.

Fig. 23 shows the damage to some of the buildings. The damage intensity shows that the tornado can be classified as F1. The damage footprint showed that it moved in a west-east direction. There was little roof damage as the majority of the roofs of non-residential buildings were of sheet material. Very few buildings had tiled roofs. The

pressure data available from the AMEDAS equipment located at Fire Station Noshiro City, 4km from the touchdown point, is shown in Fig. 24.

At the reported time of the tornado strike, the morning of Oct. 30, there was a sudden pressure drop with a simultaneous increase in ambient temperature, as is commonly associated with a tornado. A very low rainfall of the order of 4.5mm was recorded in and around the time the tornado was reported.

Concrete walls surrounding a collapsed building were also collapsed (Fig. 25). Debris was found scattered in the farm land surrounding the tornado's path (Fig. 26).

A high tornado-like wind over a roof often causes uplifting of the roof sheets. This is a common feature of tornado damage, and can be seen in Fig. 27, where the roof sheet damage shows that it may have been uplifted by suction as the tornado passed over it.

Fig.28 shows a wooden plank that had pierced a building cladding in the high tornadic wind. Other damage included damage due to falling poles that pierced building claddings. Fig. 29 shows an automobile repair

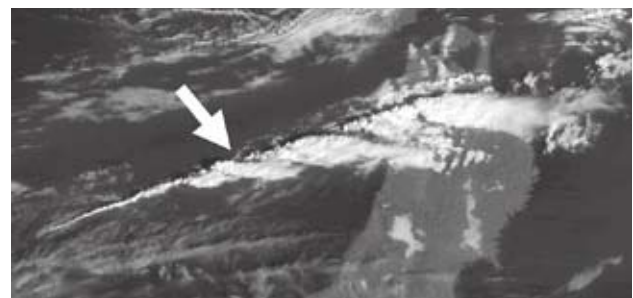


Fig. 21 Satellite Image (Oct. 30, 9 AM by JMA)

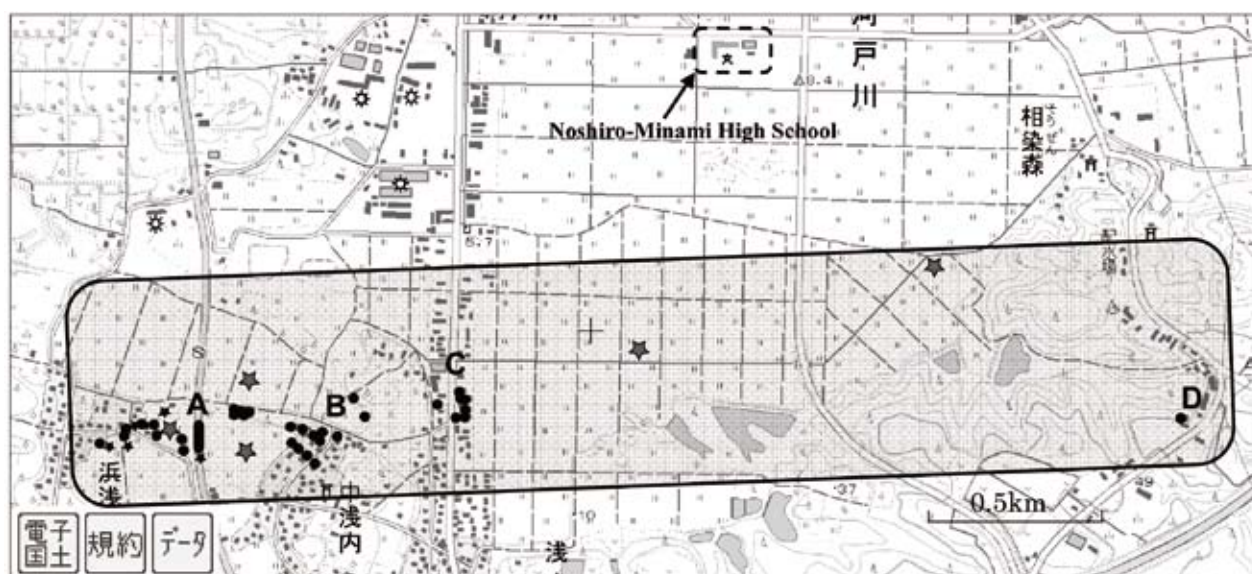


Fig. 22 Damage foot prints



(point A)



Fig. 25 Damaged Concrete Wall (point A)



(point C)
Fig. 23 Collapsed buildings



Fig. 26 Scattered debris

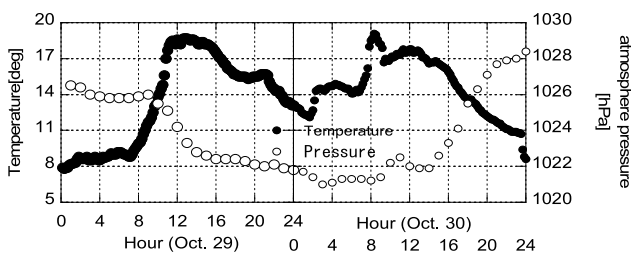


Fig. 24 Temperature and Atm. pressure Distribution at Noshiro on 29th & 30th Oct

shop. This structure suffered damage to its cladding. Moreover, a few cars were lifted up in the air by the strong wind in front of this shop.

Fig. 30 shows debris (a roof panel) that was observed near the shop in Fig. 29. This panel was around 3.0m*3.0m and it traveled around 150 m.

The instantaneous and 10-min average wind speeds recorded by the JMA as observed from Fig. 31 were about 13.2m/s and 7m/s, respectively.

Fig. 32 shows a picture from NHK News, which dealt



Fig. 27 Damaged roof steel sheet (point C)

with the tornado. In this picture, the tornado is captured clearly. This movie taken from the Noshiro-Minami high school as located in the north area of Fig. 22. In this picture, the tornado moved from right to left.

Acknowledgement

Our GCOE Group greatly appreciates afflicted people's help on our damage investigations.



Fig. 28 Cladding damaged by debris (point C and B)



Fig. 29 A few cars went up in the air (point A)



Fig. 30 Debris from dwelling

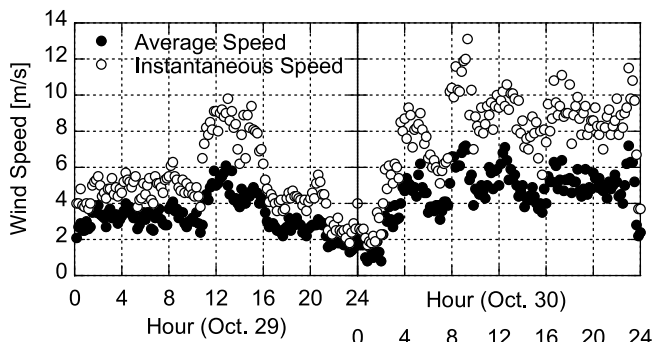


Fig. 31. Average and Instantaneous Wind Speed



Fig. 32 picture of tornado (NHK)

Recent Topics of POD in Wind Engineering

Le Thai Hoa, Tokyo Polytechnic University

INTRODUCTION

Proper orthogonal decomposition (POD) has been applied widely in many engineering topics including the wind engineering recently due to its advantage of optimum approximation of multi-variate random fields using the modal decomposition and limited number of dominantly orthogonal eigenvectors. This paper presents fundamentals of POD and its proper transformations in both the time domain and the frequency domain based on both covariance matrix and cross spectral matrix branches. Moreover, the most recent

topics and applications of POD in the wind engineering will be reviewed as follows: (1) Digital simulation of turbulence fields; (2) Analysis and synthesis of unsteady pressure fields; (3) Random response prediction of structures in turbulence and (4) Modal parameters identification of structures.

POD AND ITS PROPER TRANSFORMATIONS

POD is originally considered as optimum approximation of the multi-variate random field in which a set of orthogonal basic vectors is found out in order to expand the random

process into a sum of products of these time-independent basic orthogonal vectors and time-dependant uncorrelated random processes. Let consider the N-variate correlated random process $v(t) = \{v_1(t), v_2(t), \dots, v_N(t)\}^T$ is approximated as:

$$v(t) = x(t)^T \Theta = \sum_{i=1}^N x_i(t) \theta_i \quad (1)$$

where $x(t)$: time-dependant uncorrelated random process (principal coordinates); Θ : time-independent orthogonal modal matrix.

Covariance proper transformation in the time domain is to find covariance matrix-based eigenvalues and orthogonal eigenvectors from the zero-time-lag covariance matrix $R_v(0)$ of the random process $v(t)$:

$$R_v \Theta_v = \Gamma_v \Theta_v \quad (2)$$

where Γ_v, Θ_v : eigenvalue and eigenvector matrices $\Gamma_v = \text{diag}(\gamma_{v1}, \gamma_{v2}, \dots, \gamma_{vN})$, $\Theta_v = [\theta_{v1}, \theta_{v2}, \dots, \theta_{vN}]$, respectively. Then, the random process and its covariance matrix can be reconstructed approximately using the lowest jth-order truncated eigenvalues and eigenvectors:

$$v(t) = \Theta_v x_v(t) \approx \sum_{j=1}^{\tilde{N}} \theta_{v_j} x_{v_j}(t); R_v = \Theta_v \Gamma_v \Theta_v^T \approx \sum_{j=1}^{\tilde{N}} \theta_{v_j} \gamma_{v_j} \theta_{v_j}^T,$$

where \tilde{N} : number of truncated covariance modes ($\tilde{N} \ll N$).

Similarly, spectral proper transformation in the frequency domain is to find spectral eigenvalues and spectral orthogonal eigenvector through the cross spectral density matrix $S_v(n)$ of the random process $v(t)$:

$$S_v(n) \Psi_v(n) = \Lambda_v(n) \Psi_v(n) \quad (3)$$

where $\Lambda_v(n), \Psi_v(n)$: spectral eigenvalue and eigenvector matrices $\Lambda_v(n) = \text{diag}(\lambda_{v1}(n), \lambda_{v2}(n), \dots, \lambda_{vN}(n))$ and $\Psi_v(n) = [\psi_{v1}(n), \psi_{v2}(n), \dots, \psi_{vN}(n)]$, respectively. Accordingly, cross spectral density matrix of random process can be approximated as follows:

$$S_v(n) = \Psi_v(n) \Lambda_v(n) \Psi_v^T(n) \approx \sum_{j=1}^{\tilde{N}} \psi_{v_j}(n) \lambda_{v_j}(n) \psi_{v_j}^T(n) \quad (4)$$

where \tilde{N} : number of truncated spectral modes ($\tilde{N} \ll N$).

SIMULATION OF TURBULENCE FIELDS

The spectral proper transformation can be applied to simulate the multi-variate turbulence fields. For example, simulation of fluctuating wind speeds $u(t)$, $w(t)$ at 30-nodes line-like structure is required at sampling rate of 1000Hz for time interval 100 seconds. Targeted auto power spectral densities of u -, w -components are used the Kaimail's and Panofsky's empirical formula. Coherence function is used by Davenport's exponentially empirical model. First five spectral eigenvalues $\lambda_1(n) \div \lambda_5(n)$ and the first spectral mode on frequency band $0.01 \div 10\text{Hz}$ is shown in Figure 1 and Figure 2.

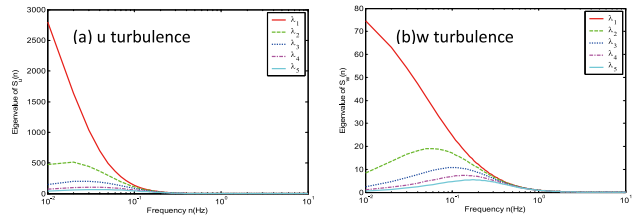


Fig.1 First five spectral eigenvalues

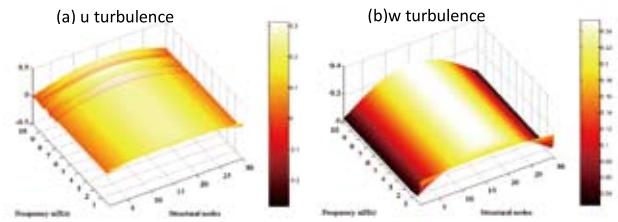


Fig.2 First spectral mode

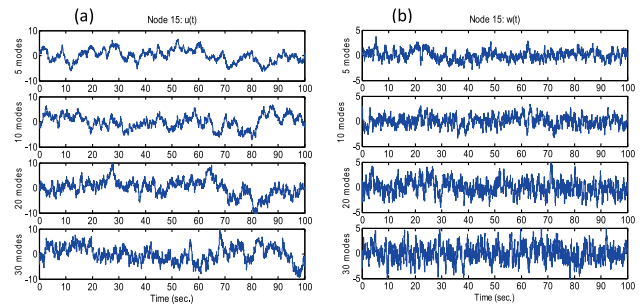


Fig.3 Simulated time series of fluctuating wind speeds u (a) and w (b) at $U=20\text{m/s}$ (Node 15)

ANALYSIS AND SYNTHESIS OF UNSTEADY PRESSURE FIELD

Unsteady pressure field on typical square prism $B/D=1$ has been used for demonstration. Pressure has been measured at lower surface in chordwise directions from position 1 to position 10 under some turbulence flows. Figure 4 shows normalized pressure distribution and power spectral density at some chordwise positions. Spectral peak of 4.15Hz represents to Karman vortex's frequency at the wake of square prism.

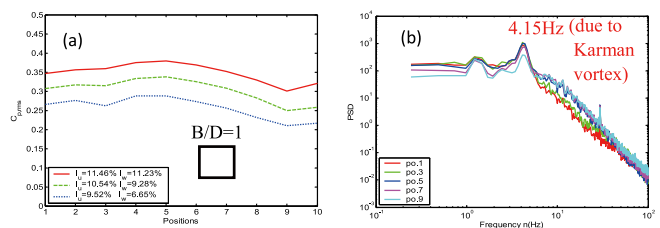


Fig.4 Normalized pressure (a) and power spectral densities (b)

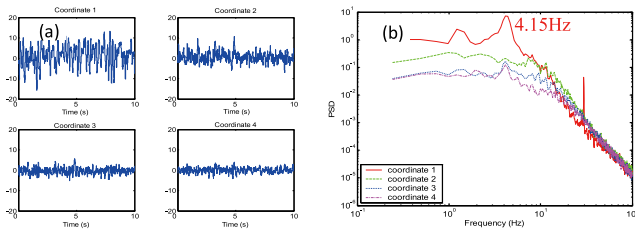


Fig.5 First four principal coordinates (a) and power spectra (b)

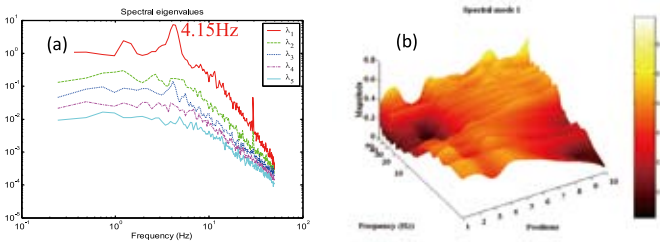


Fig.6 First five spectral eigenvalues and first spectral mode

As can be seen from Figure 5 and Figure 6, only the first covariance matrix-based principal coordinate and also the first spectral matrix-based eigenvalue contain the frequency of the Karman vortex event. In the other word, The first principal coordinate and spectral eigenvalue in these studies have represented to physical phenomenon of the experimental model.

RANDOM RESPONSE ANALYSIS OF STRUCTURES

Random response of structures under turbulence flows can be formulated either in the time domain or the frequency domain using the proper transformation branches. By using POD, random buffeting forces can be decomposed under the concept of orthogonal loading modes, after that are combined with structural modes to estimate the response of structures. Random response of cable-stayed bridge under turbulence has been taken into account for numerical example. Some results of the buffeting response prediction in the frequency domain and the time domain have been expressed in Figure 7 and Figure 8.

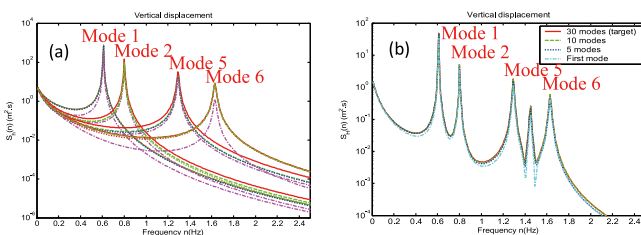


Fig.7 Power spectra of generalized (a) and global responses (b) of vertical displacement

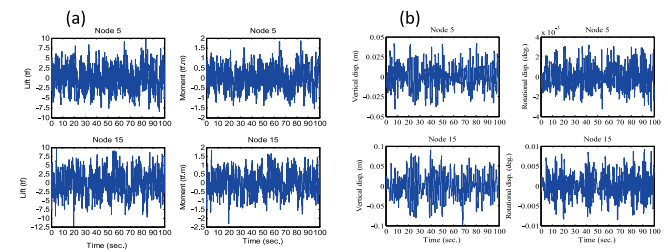


Fig.8 Time series of global forces (a) and global response (b) of nodes 5 & 15 at mean velocity $U=20\text{m/s}$

The advantage of POD for predicting the random response of structure is that only first few covariance modes or spectral modes of random loading can be used for enough accuracy of response estimation.

MODAL PARAMETERS IDENTIFICATION

Modal parameters (natural frequencies, damping ratios and mode shapes) of operational and experimental structures can be identified in the frequency domain and the time domain using the POD via ambient vibration data. Measured data also are organized under any form of spectral matrix, covariance matrix or data themselves (Hankel matrix). Here, modal parameters identification in the frequency domain of 5-storey steel building under ambient data is presented (Figure 9). Figure 10 shows the spectral eigenvalues and first eigenvector of cross spectral matrix of output response.

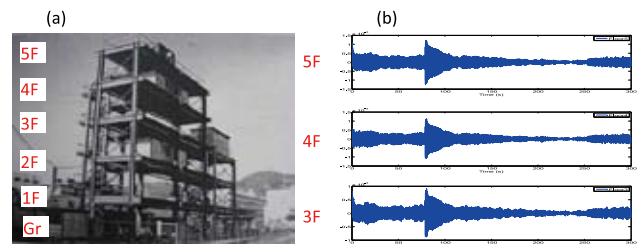


Fig.9 5-storey structure (a) and integrated displacements (b)

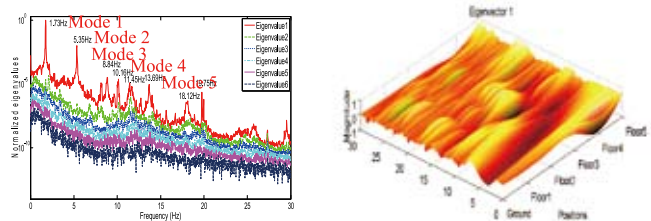


Fig.10 Spectral eigenvalues (a) and first spectral mode (b)

Accordingly, natural frequencies and damping ratios can be extracted from the first spectral eigenvalue, whereas the mode shapes from the first spectral eigenvector.

Vibration Control of Stay-Cable Using Magneto Rheological Damper

Zhehua Wu, Tokyo Polytechnic University



As the most important structural components in cable-supported bridges, stay cables are vulnerable to vibrations with large amplitudes due to relate small mass, low internal structural damping and high flexibility. A number of methods have been proposed to mitigate cable vibrations, such as cable cross tie system, aerodynamic cable surface treatment and damper cable control. However, each has limitations in suppressing the longer cable vibration. As one of smart control devices, magneto-rheological (MR) dampers have significant potential to advance the acceptance of structural control as a viable means for dynamic hazard mitigation. The following paragraph will focus on the field of control of cable vibration by using MR dampers.

1.Experimental Research

The full-scale experiment using MR dampers was carried out for mitigation cable vibration. Fig.1 shows the dampers were installed on the 154m-long cable near the anchorage in the 3rd QianJiang cable-stayed bridge,China. MR dampers applied constant current are examined by a series of free vibration tests and compared to that of using oil dampers.

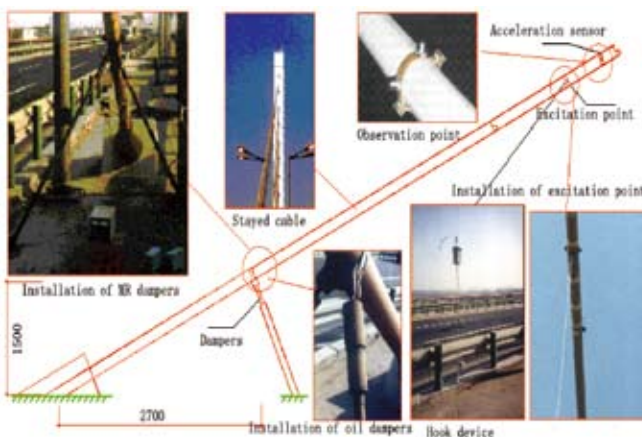


Fig. 1 Experiment setup

The displacement signal is driven by harmonic planar loads, filtered through wavelet decomposition and

transformed by Hilbert. The relationship between system equivalent modal damping ratios, resonant frequencies, applied voltages and displacement responses of the cable was pursued. Fig.2 shows that MR dampers can more significantly reduce cable vibration than oil dampers do. The resonant frequencies of the cable installed MR dampers have a little change as shown in Fig. 3.

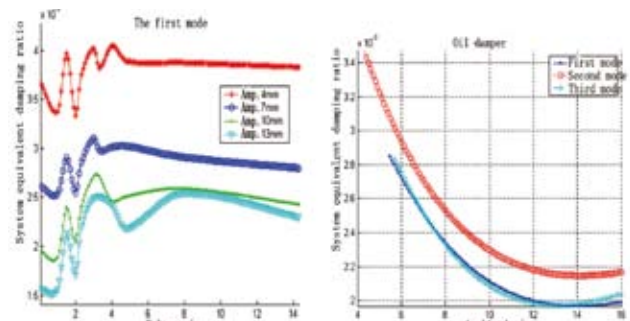


Fig. 2 System equivalent modal damping ratio

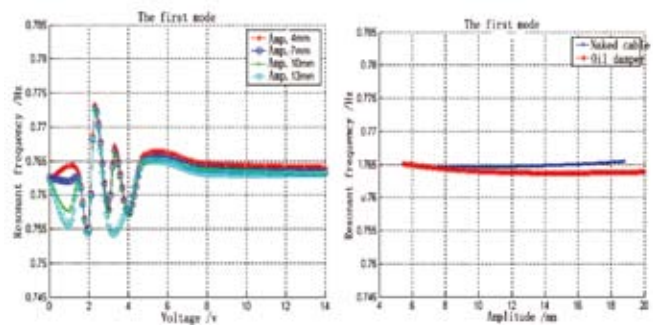


Fig. 3 Resonant frequency

A theoretical model for the cable damper system is formulated by accounting for the cable inclination and sag effect based on the Hamilton's principle. The motion of the cable was computed by using a finite series approximation with the Galerkin method. A static deflection shape as an addition shape function improved the sine series convergence. A nonlinear hysteretic biviscous model is identified for the experimental MR dampers.

Tab. 1 shows the similar phenomenon and conclusions between experiment and numerical simulation.

Table. 1 System equivalent modal damping ratio and resonant frequency

Parameters	The 1st mode		The 2nd mode		The 3rd mode	
	Exp.	Sim.	Exp.	Sim.	Exp.	Sim.
Damping ratio (%)	0.46	0.49	0.39	0.56	0.38	0.57
Frequency (Hz)	0.76	0.77	1.51	1.53	2.27	2.28

2.Theoretic Research

A stay cable incorporated with MR dampers exhibits pronounced nonlinearity. The Spencer photometric model is used for MR dampers. Fig. 4 shows the dynamic system of a cable and MR damper.

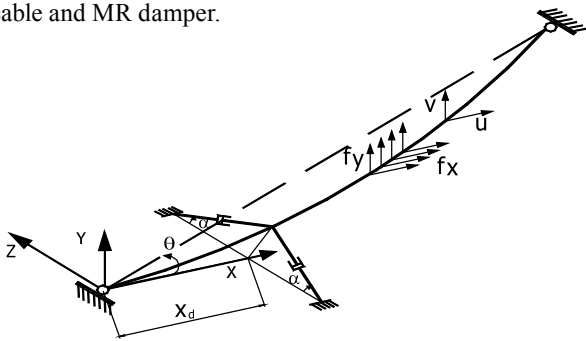


Fig. 4 Mathematic model of cable with attached damper

Evolution principle for controlling effect is based on root mean square (RMS) of structural response. The mitigation performance of damper contribution measured by displacement RMS integrated the whole length of cable and the whole time is expressed by:

$$v_{RMS} = \sqrt{\frac{\int_0^{t_f} \int_0^l v^2(x,t) dx dt}{t_f}} \tag{1}$$

Where t_f is the total time of vibration response, $v(x,t)$ is the displacement response of cable. The relationship between displacement RMS, the optimal marker of MR damper, the mounting position, the applied voltage, the first frequency of cables (tensile force, length and mass per unit length), Irvine parameter, and excited loads (type, frequency and amount) are studied. To compare MR damper to oil damper, the ratio of displacement RMS is defined as:

$$v_{RRMS} = \frac{v_{RMS}^{MR}}{v_{RMS,opt}^{OIL}} \tag{2}$$

Where v_{RMS}^{MR} and $v_{RMS,opt}^{OIL}$ are displacement RMS using MR and the optimal oil damper respectively. Fig. 5 shows the mitigation effect of the cable is equal to the optimal oil dampers do. MR damper is a type of fail-safe device and can offer comparatively large equivalent model damping ratio without applied voltage. There is optimum voltage on which the maximum modal damping ratio can be achieved.

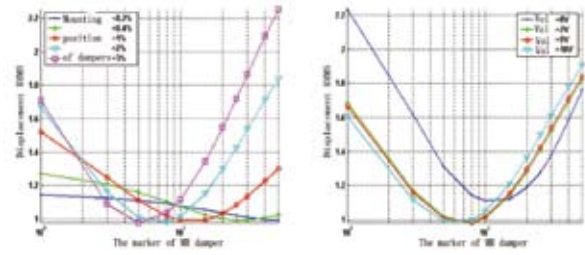


Fig. 5 Mitigation effect of MR damper under random loads

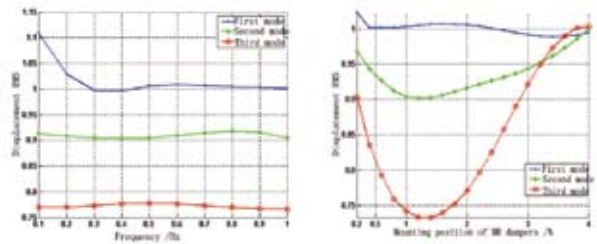


Fig. 6 The frequency mitigation range of MR dampers compared with the optimal viscous damper in the first mode

Fig. 6 shows the dynamic control range of MR damper is sufficiently wide and can be more effective in first three frequency modes than oil dampers do.

Based on equivalent RMS cable deflection criteria, the simplifying model is established for MR damper passive control. The damper force is expressed as:

$$F_d = K_{eq}x_d + C_{eq}\dot{x}_d \tag{3}$$

Where K_{eq} and C_{eq} are equivalent stiffness coefficient and equivalent viscous damping coefficient respectively, and x_d and \dot{x}_d are displacement and velocity of damper respectively. The simplifying model not only has the similar effect of mitigation to the Spencer model but also reveal the laws of energy dissipation criteria for MR dampers much better. Fig. 7 shows the mechanics performance of MR dampers is relate to applied voltage, displacement amplitude and frequency, and explains the difference in dynamic response. Using partial least squares in conjunction with the chebyshev polynomial representation, the expression for the simplifying model is built, and is provided to determine the optimal MR damper marker.

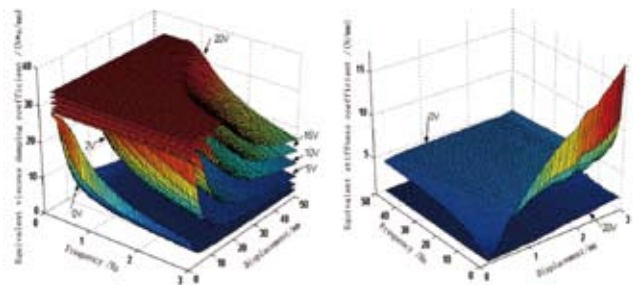
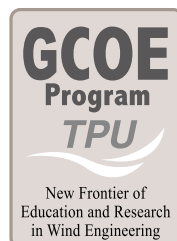


Fig.7 Identification of equivalent stiffness coefficient and equivalent viscous damping coefficient



Executors of the Global COE Program New Frontier of Education and Research in Wind Engineering

Director			
Yukio Tamura	Professor	Director of Global COE Program	yukio@arch.t-kougei.ac.jp
Ahsan Kareem	Professor	Technology related to EVO	kareem@nd.edu
Masaaki Ohba	Professor	Design method for natural/cross ventilation	ohba@arch.t-kougei.ac.jp
Takashi Ohno	Professor	Wind resistant construction	ono@arch.t-kougei.ac.jp
Ryuichiro Yoshie	Professor	Heat exhaust and air pollution in urban area	yoshie@arch.t-kougei.ac.jp
Kunio Mizutani	Professor	Natural ventilation dehumidifying system	mizutani@arch.t-kougei.ac.jp
Takeshi Ohkuma	Invited Professor	Wind resistant design method	ohkuma@arch.kanagawa-u.ac.jp
Masahiro Matsui	Professor	Engineering simulator for tornado-like flow	matsui@arch.t-kougei.ac.jp
Akihito Yoshida	Associate Professor	Development of wind response monitoring network	yoshida@arch.t-kougei.ac.jp

Wind Engineering Research Center Graduate School of Engineering Tokyo Polytechnic University

1583 Iiyama, Atsugi, Kanagawa, Japan 243-0297

TEL & FAX : +81-046-242-9658

URL : <http://www.wind.arch.t-kougei.ac.jp/>